NMR studies of methane and hydrogen in microporous materials

Yu Ji, J.A. Hamida, Yibing Tang, and N.S. Sullivan

Department of Physics, University of Florida, Gainesville, FL, USA
E-mail: sullivan@phys.ufl.edu

We review the results of nuclear magnetic resonance studies of the molecular dynamics of the quantum gases HD and CH_4 adsorbed in the cages of microporous structures. Measurements of the variation of the nuclear spin-lattice and nuclear spin-spin relaxation times with temperature provide detailed information about the translational and rotational dynamics of the adsorbed molecules over a wide temperature range.

1. Introduction

The absorption and dynamics of H_2 and CH_4 among other light gases (CO, CO_2, N_2…) when confined to the internal cages of mesoporous structures has received great interest in recent years because of the potential use of these mesoporous materials (MOFs, MCM, zeolites...) for the storage and transport of commercially important gases [1–7]. The efficiencies of various nanoporous and microporous materials for storage and ease of removal depend crucially on the thermodynamic properties of these gases at or near the surfaces of the chosen materials [8–12]. These properties and the characteristic dynamics are also important in the development of methods for CO_2 sequestration [13–15]. There is considerable documentation in the literature about the total absorption properties of light gases (such as hydrogen and methane) on various porous materials but there is little information about the detailed dynamics of the gases in the confined geometries or about their interactions with the walls of the confinement. One of the great advantages of the use of NMR techniques is that they can address this need. In this paper we review recent applications of NMR methods to study the dynamics of CH_4 and HD in microporous materials [16–19].

2. Experimental methods

Careful NMR techniques can be very powerful tools for measuring the dynamics of molecules in condensed matter systems. The motion of the molecules modulates the nuclear dipole-dipole interactions between the spins of the molecules as well as the interactions between the spins of the mobile molecules and the magnetic spins in the walls of the porous adsorbers. The Fourier components of these fluctuations at $\omega = \omega_L$, the nuclear Larmor frequency, can induce transitions between the nuclear spin levels of the molecules and this will determine the nuclear spin-lattice relaxation times. In order to calculate the relaxation times we follow Cowan [20] and express the dipolar spin-spin interactions in terms of irreducible components

$$H_{\text{dip}} = \sum_{m=-2}^{2} D_m, \tag{1}$$

where for like spins

$$D_m = \frac{\mu_0}{4\pi} \frac{\hbar^2 \gamma^4}{\sqrt{5}} \sum_{ij} Y_2^{-m}(\Omega_{ij}) T_2^m(ij)/r_{ij}^3, \tag{2}$$

μ_0 is the permeability of free space, γ is the nuclear gyromagnetic ratio of the nucleus, $Y_2^m(\Omega_{ij})$ is the spherical harmonic for the angles $\Omega_{ij} = (\theta_{ij}, \varphi_{ij})$ specifying the orientation of the vector r_{ij} with respect to the applied magnetic field, θ_{ij} is the polar angle and φ_{ij} is the azimuthal angle for the vector r_{ij}. The $T_2^m(ij)$ are irreducible nuclear spin operators that transform under rotation in the same manner as the spherical harmonics:

$$T_2^0(ij) = I_i \cdot I_j - 3I_i^z I_j^z, \tag{3}$$

$$T_2^1(ij) = \sqrt{\frac{3}{2}}[I_i^z I_j^+ + I_i^+ I_j^z], \tag{4}$$

$$T_2^2(ij) = -\sqrt{\frac{3}{2}} I_i^+ I_j^+, \tag{5}$$

with $T_2^{-m}(ij) = (-)^m [T_2^m(ij)]^\dagger$.

In the simplest cases where a single correlation time for the fluctuations dominates one can obtain a direct measure of the microscopic motion:

$$\frac{1}{T_1} = \frac{2}{3} M_2 \sum_{n=1,2} n^2 J_n(n\omega_L), \qquad (6)$$

where M_2 is the second moment of the nuclear spin interactions and $J_n(\omega)$ is the Fourier component of the autocorrelation functions for the dipolar interactions given by $G_n(t) = \left\langle Y_{2n}^*(t) Y_{2n}(0) \right\rangle$.

This simple case often occurs for the translational and rotational diffusion of molecules in condensed phases. If the motion is characterized by a unique correlation time, τ_c, as for example, given by the microscopic jump time from one lattice site to a neighboring site in the case of translational diffusion, the NMR measurements can determine the correlation time and thus the diffusion constant ($D \sim z a_0^2 \tau_c^{-1}$, where a_0 is the lattice spacing and z the coordination number). These times inferred from NMR measurements can be compared with those deduced from neutron scattering measurements. In addition to the spin-lattice relaxation time one can also measure the nuclear spin-spin relaxation times, T_2. These times are determined by the Fourier component at close to $\omega = 0$. Specifically,

$$\frac{1}{T_2} = \frac{1}{4} \sum_{n=-2}^{2} (6 - n^2) J_n(n\omega_L). \qquad (7)$$

In the case of a unique correlation time for the motion, as is often the case for motions associated with quantum jumping in adsorbed gases we can simplify Eqs. (6) and (7). For rapid motion where the correlation time $\tau_c \ll \omega_L^{-1}$ we have

$$\frac{1}{T_1} = \frac{1}{T_2} = \frac{10}{3} M_2 \tau_c. \qquad (8)$$

In the opposite case of slow motions, for which $\tau_c \ll \omega_L$, we have

$$\frac{1}{T_1} = \frac{4}{3} \frac{M_2}{\omega_L^2 \tau_c}, \qquad (9)$$

$$\frac{1}{T_2} = M_2 \tau_c. \qquad (10)$$

In many cases at low temperatures there can be several sources of excitations; phonons, spin-interactions, quantum diffusion, and the different interactions can form weakly coupled energy reservoirs. In this situation the relaxation will depend on the couplings between the respective energy baths associated with these excitations as illustrated in Fig. 1 where R_{XY} represents the relaxation rate between baths X and Y.

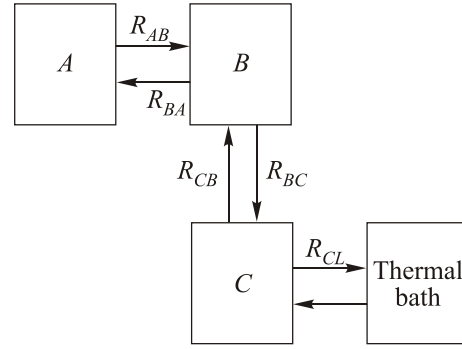If the energy baths can attain thermal equilibrium in a time short compared to the relaxation couplings between

Fig. 1. Illustration of different weakly coupled energy baths designated by A, B and C where the weakest coupling is the vertical path between B and C.

the baths, the relaxation time observed experimentally will vary with changes in the heat capacities of the individual baths. In Fig. 1 we show the case where the coupling R_{BC} is the slowest (or weakest) connection for the energy flow. In this case the observed relaxation time will be

$$T_{1,\text{observed}} = \frac{C_A + C_B}{C_B} T_{BC}, \qquad (11)$$

where C_A, C_B are the heat capacities of baths A and B. When this situation occurs, the experiments often show a two-stage relaxation process: (i) a short-time relaxation as an energy bath comes into internal thermal equilibrium after a disturbance, and (ii) a long-time component to the relaxation determined by cross-relaxation between different energy baths.

3. Experimental observations

Prior to the NMR studies the mesoporous substrate materials were all first characterized by measuring the adsorption isotherm at a fixed temperature. A typical example for methane adsorbed on zeolite is shown in Fig. 2 for a sample maintained at 77 K. Small gas volumes are adsorbed sequentially and the equilibrium pressure at each step is recorded as one point on the graph. The observation of at least two steps in the isotherm is a measure of a high-quality surface.
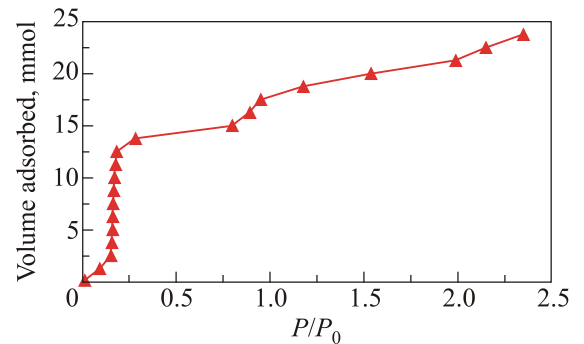

Fig. 2. Experimental isotherm for methane on zeolite 13X. (After Fig. B1 from Ref. 19.)

3.1. Adsorbed methane

Studies of the relaxation of the nuclear spins of methane adsorbed on zeolite 13X show unexpected features, namely the existence of two prominent peaks in the temperature dependence below 65 K. These peaks are believed to result from the existence of rotational energy levels associated with the tetrahedral molecules, associated with the A, E and T representations of the tetrahedral group T_d. The ground state is the A-state with total nuclear spin $I = 2$ and the next level is the T-state with $I = 1$. The E-state with $I = 0$ is not relevant for the nuclear spin relaxation rate. For adsorbed molecules the E-state can split into separate A- and T-states for sites with trigonal symmetry as is the case for molecules near some of the faces in the zeolite cages. The solid red line shown in Fig. 3 is a fit for two distinct T-states using Eq. (10) with heat capacities

$$C_A = \frac{3}{2} N g_A k_B, \tag{12}$$

$$C_{T_i} = N g_{T_i} k_B \left[\left(\frac{\Delta_i}{2T} \right)^2 \operatorname{sech}^2 \left(\frac{\Delta_i}{2T} \right) \right] \tag{13}$$

for the A- and T_i-states, respectively. g_A and g_{T_i} are the degeneracies of the A- and T_i-states, respectively. The best fit is obtained for two T-states with energies $\Delta_1 = 25$ K and $\Delta_2 = 55$ K, as represented by the red line in Fig. 3.

At high temperatures one observes a straightforward thermal activation for the nuclear spin-lattice relaxation times and that is expected for the translational degrees of freedom of the molecules. The best description of the experimental points is obtained using Eq. (6) with a Lorentzian spectral density of the form

$$J(n\omega) = \frac{\tau}{1 + (n\omega\tau)^2} \tag{14}$$

with the correlation time τ given by the molecular jump time

$$\tau = \tau_0 e^{E_{act}/T} \tag{15}$$

with $\tau_0 = 7.1 \cdot 10^{-13}$ s and $E_{act} = (2600 \pm 260)$ K. This fit is given by the green line of Fig. 3. The activation energy compares favorably with the results of Monte Carlo simulations reported by Yashoanth *et al.* [21]. The rounded minimum at 78 K in the solid green curve of Fig. 3 is the BPP minimum [22] that arises when the Larmor frequency and the molecular motional frequencies are equal.

3.2. HD on zeolite 13X and Z-MOF

The dynamics of HD molecules has been studied for two types of structures, zeolite 13X and the metal organic framework Z-MOF. HD was explored rather than H_2 because of the difficulties associated with the ortho-para conversion of H_2 and consequent uncertainty of the ortho-H_2 concentration as a sample ages. The nuclear relaxation data for HD is also more straightforward to interpret because only translational degrees of freedom are relevant.

At high temperatures we see a simple thermal activation of the translational diffusion of the molecules as shown in Fig. 4. The solid red line of Fig. 4 is found from Eq. (9) with $\tau_c = \tau_0 e^{E_{act}/T}$, $\tau_0 = 6.7 \cdot 10^{-13}$ s and $E_{act} = (73 \pm 3)$ K. These values for τ_c correspond to a translational diffusion constant of $D = (8.2 \pm 2.8) \cdot 10^{-6}$ cm^2/s at $T = 19.5$ K which is comparable to the values observed by Coulomb *et al.* [23] using neutron scattering techniques.

One of the unexpected results of the studies was the observation of peaks in the dependence of the nuclear spin-lattice relaxation times at low temperatures for HD on zeolite. This behavior is illustrated in Fig. 5. These peaks suggest that there is a discreet set of energy levels for the translational motion and that these levels contrib-
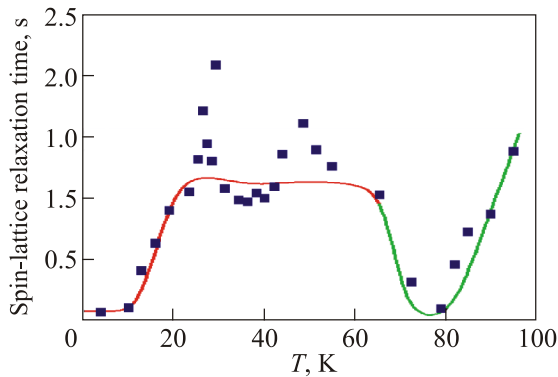

Fig. 3. (Color online) Variation with temperature of the spin-lattice relaxation times of methane adsorbed on zeolite. The solid red line represents the contribution of the Schottky specific heats of the rotational states of methane, and the solid green line is the calculated variation for thermally activated translational motion in the zeolite cage. (Reproduced with permission from Fig. 4 of Ref. 16.)
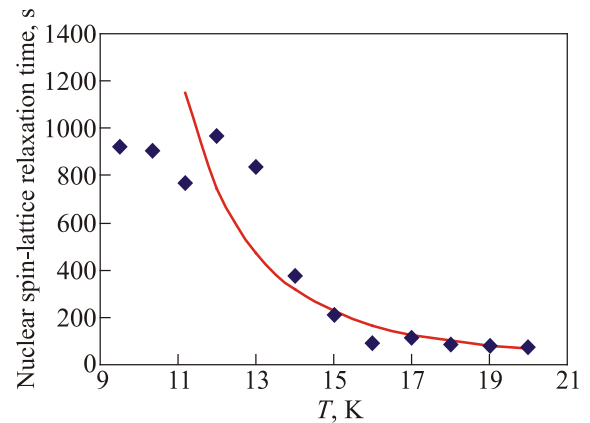

Fig. 4. Dependence of the nuclear spin-spin relaxation times with temperature for HD adsorbed on zeolite 13X. The solid line corresponds to a calculated variation for a thermal activation energy of (72 ± 3) K. (After Fig. 9 of Ref. 19.)
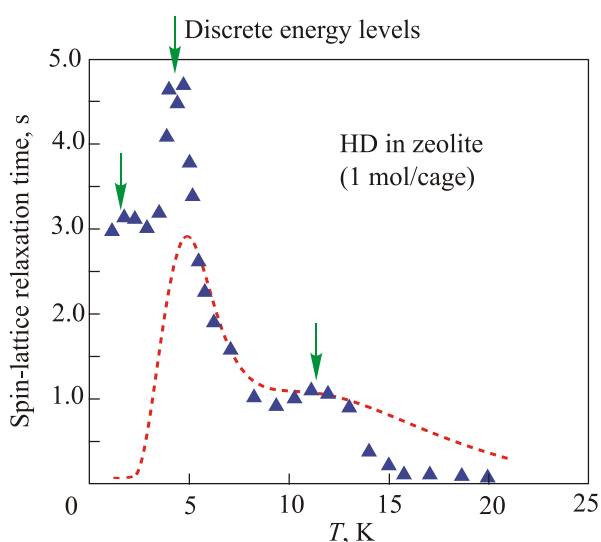
Fig. 5. Observed variation of the nuclear spin-lattice relaxation times of HD in zeolite 13X at low temperatures. The broken line shows the Schottky contribution for energy levels at 7.5 and 19.6 K. (Reproduced with permission from Fig. 3 of Ref. 17.)

ute to peaks in the heat capacity. From Eq. (6) we expect a corresponding set of peaks in the values of T_1 at the temperatures corresponding to those energies. For a particle in a potential well, the energy levels are found to be $E_{n,l} = \hbar^2 k_{n,l}^2 / 2md$, where the $k_{n,l}$ are the spherical Bessel function, $j^l(kr)$ [24]. The effective value of d is the diameter of the cage minus twice the hard core radius of the molecule. The lowest energy levels are found to be 1.9, 4.4, 5.6, 7.4 K [18].

4. Conclusion

Studies of the nuclear spin relaxation times of molecules adsorbed in mesoporous structures can provide direct non-invasive measurements of the translational and rotational dynamics of the molecules constrained to the pores of the structures. The activation energies observed for both HD and CH_4 measurements appear to be in reasonably good agreement with results reported from studies using other techniques. The most unusual feature was the observation of relatively sharp peaks in the relaxation times at low temperatures for the translational energies. These peaks are close to the energy values expected for the quantization of the translational motion for a particle in the pores, but further studies are needed to verify this interpretation.

Acknowledgments

1. A. Züttel, *Materials Today* **6**, 24 (2003).
2. D.P. Broom, *Hydrogen Storage Materials: Characterization of their Properties*, Springer, SBM (2011).
3. G. Chen, L.N. Zakharov, M.E. Bowden, A.J. Karkamkar, S.M. Whittemore, E.B. Garner, T.C. Mikulas, D.A. Dixon, T. Autrey, and S.-Y. Liu, *J. Amer. Chem. Soc.* **137**, 134 (2015).
4. T.A. Makal, J.-R. Li, W. Lu, and H.-C. *Zhou, Chem. Soc. Rev.* **41**, 7761 (2012).
5. C.M. Simon, J. Kim, D.A. Gŏmez-Gualdrŏn, J.S. Camp, Y.G. Chung, R.L. Martin, R. Mercado, M.W. Deem, D. Gunter, M. Haranczyk, D.S. Sholl, R.Q. Snurr, and B. Smit, *Energy Environ. Sci.* **8**, 1190 (2015).
6. D.A. Gómez-Gualdrón, C.E. Wilmer, O.K. Farha, J.T. Hupp, and R.Q. Snurr, *J. Phys. Chem. C* **118**, 6941 (2014).
7. A.V. Vakhrushev and M.V. Suyetin, *Nanotechnology* **20**, 125602 (2009).
8. M. Bienfait, P. Zeppenfeld, N. Dupont-Pavlovsky, M. Muris, M. Johnson, T. Wilson, M.D. Pies, and O. Vilches, *Physica B: Condensed. Matter* **350**, E423 (2004), Proc. Third European Conf. on Neutron Scattering.
9. G. Bomchil, A. Hüller, T. Rayment, S.J. Roser, M.V. Smalley, R.K. Thomas, J.W. White, and A.D. Buckingham, *Philos. Trans. Royal Soc. Ln. Series B, Biological Sciences* **290**, 537 (1980).
10. M.K. Rana, H.S. Koh, H. Zuberi, and D.J. Siegel, *J. Phys. Chem. C* **118**, 2929 (2014).
11. E. Poirier and A. Dailly, *Nanotechnology* **20**, 204006 (2009).
12. C.O. Aren, S. Chavan, C.P. Cabello, E. Garrone, and G.T. Palomino, *Chem. Phys. Chem.* **11**, 3237 (2010).
13. A. Macario, A. Katovic, G. Giordano, F. Iucolano, and D. Caputo, *Microporous Mesoporous Mater.* **81**, 139 (2005).
14. C. Xu and N. Hedin, *Materials Today* **17**, 397 (2014).
15. S.-H. Liu, W.-C. Hsiao, and W.-H. Sie, *Adsorption* **18**, 431 (2012).
16. Y. Ji, J.A. Hamida, and N.S. Sullivan, *J. Low Temp. Phys.* **158**, 509 (2010).
17. Y. Ji, N.S. Sullivan, and J.A. Hamida, *J. Low Temp. Phys.* **162**, 121 (2011).
18. Y. Ji, Y. Tang, J.A. Hamida, and N.S. Sullivan, *J. Phys.: Conf. Ser.* **400**, 012024 (2012).
19. Y. Ji, N.S. Sullivan, Y. Tang, and J.A. Hamida, *Materials* **6**, 2464 (2013).
20. B.P. Cowan, *Nuclear Magnetic Resonance and Relaxation*, Cambridge University Press, Cambridge, UK (1997).
21. S. Yashonanth, J.M. Thomas, K. Nowak, and A.K. Cheetham, *Nature* **331**, 601 (1988).
22. N. Bloembergen, E.M. Purcell, and R.V. Pound, *Phys. Rev.* **73**, 679 (1948).
23. J.P. Coulomb, N. Flouquet, N. Dufau, P. Llewellyn, and G. Andre, *Microporous Mesoporous Mater.* **101**, 271 (2007).
24. S. Gasiorowicz, *Quantum Physics*, John Wiley and Sons, New York (1974).